Hydrothermal Synthesis and Characterization of Hexavanadium Polyoxo Alkoxide Anion Clusters: Crystal Structures of the Vanadium(IV) Species $Ba[V_6O_7(OH)_3\{(OCH_2)_3CCH_3\}_3]\cdot 3H_2O$ and $Na_2[V_6O_7\{(OCH_2)_3CCH_2CH_3\}_4]$, of the Mixed-Valence Complex $(Me_3NH)[V^{IV}_5V^{V}O_7(OH)_3\{(OCH_2)_3CCH_3\}_3]$, and of the Fluoro Derivative $Na[V_6O_6F(OH)_3\{(OCH_2)_3CCH_3\}_3]\cdot 3H_2O$

M. Ishaque Khan,† Qin Chen,† Hakon Höpe,‡ Sean Parkin,‡ Charles J. O'Connor,§ and Jon Zubieta*,†

Departments of Chemistry, Syracuse University, Syracuse, New York 13244, University of California at Davis, Davis, California 95616, and University of New Orleans, New Orleans, Louisiana 70148

Received November 24, 1992

The hydrothermal reactions of vanadium oxide precursors with trialkoxy ligands of the class $(HOCH_2)_3CR$ (R = CH_3, CH_2CH_3) yield polyalkoxyoxovanadium clusters with a hexametalate core, $Ba[V_6O_7(OH)_3\{(OCH_2)_3CCH_3\}_3]\cdot 3H_2O$ (**1**), $Na_2[V_6O_7\{(OCH_2)_3CCH_2CH_3\}_4]$ (**2**), $(Me_3NH)[V_6O_7(OH)_3\{(OCH_2)_3CCH_3\}_3]$ (**3**), and $Na[V_6O_6F(OH)_3\{(OCH_2)_3CCH_3\}_3]\cdot 3H_2O$ (**4**). Cluster **1** is a fully-reduced V(IV) species in which nine doubly bridging oxo groups of the parent $\{V_6O_{19}\}$ core have been substituted by alkoxy oxygen donors of the three trialkoxy ligands. The structure of **3** is grossly similar to that of **1**, with differences in metrical parameters reflecting the presence of one oxidized V(V) site in the metal core of **3**. The fully reduced cluster **2** exhibits complete substitution of the doubly-bridging oxo groups of the parent core by 12 ligand alkoxy donors. The tendency of polyvanadium oxide clusters to encapsulate a variety of guest molecules or ions is demonstrated by the structure of **4**, in which the central μ_6-oxo group of the parent core has been substituted by a μ_3-fluoride, resulting in a considerably distorted $\{V_6O_6(\mu_3\text{-}F)(\mu_2\text{-}OH)_3(\mu_2\text{-}OR)_9\}$ core. Crystal data for **1**: hexagonal space group $P6_3mc$, a = 13.707(1) Å, c = 9.647(2) Å, V = 1569.7(2) Å^3, Z = 2, D_{calc} = 2.140 g cm^{-3}; structure solution and refinement based on 399 reflections converged at R = 0.0576. Crystal data for **2**: cubic space group $Fd3$, a = 19.202(4) Å, V = 7080(1) Å^3, Z = 8, D_{calc} = 1.749 g cm^{-3}; 293 reflections, R = 0.0509. Crystal data for **3**: hexagonal space group $P6_3mc$, a = 12.792(3) Å, c = 10.692(2) Å, V = 1515.2(6) Å^3, Z = 2, D_{calc} = 1.929 g cm^{-3}; 651 reflections, R = 0.0410. Crystal data for **4**: hexagonal space group $P6_3mc$, a = 12.977(1) Å, c = 10.160(1) Å, V = 1481.7(2) Å^3, Z = 2, D_{calc} = 2.020 g cm^{-3}; 379 reflections, R = 0.0371.

Introduction

While the chemistries of the isopolyanions, $[M_xO_y]^{n-}$, and the heteropolyanions, $[E_aM_xO_y]^{n-}$, of the early transition elements have been extensively developed,[1-3] their coordination compounds—clusters in which one or more peripheral oxo groups have been replaced by organic ligands, $[L_nM_xO_y]^{m-}$ or $[L_nE_aM_xO_y]^{m-}$—have only recently witnessed systematic investigations.[4-6] The coordination chemistry of the isopolymetalates has been shown to be dominated by species containing organic ligands with oxygen donor groups—of which the formylated species $[(HCO)_2Mo_8O_{26}]^{6-}$,[7] the alkoxy derivative $[H_2Mo_8O_{24}(OR)_2]^{4-}$,[8] and the acetal derivatives $[RMo_4O_{15}X]^{3-}$[9,10] are characteristic—and/or with nitrogen donors.[11-17] The polyoxoalkoxometalates $[M_aO_b(OR)_c]^{x-}$ and their derivatives with other organic ligands represent a major subclass of coordination compounds of the soluble metal oxide clusters.[18] These compounds are of some interest not only by virtue of their diverse structures and versatility as synthetic precursors but also as a consequence of their relationship to both metal oxides and the oligomeric metal alkoxides, a second major class of inorganic materials.[19-24] While the polyoxoalkoxometalates thus provide examples of soluble metal

† Syracuse University.
‡ University of California at Davis.
§ University of New Orleans.

(1) (a) Pope, M. T. *Heteropoly and Isopoly Oxometalates*; Springer Verlag: New York, 1983. (b) Pope, M. T. In *Comprehensive Coordination Chemistry*; Wilkinson, G., McCleverty, J. A., Gillard, R., eds., Pergamon Press: Oxford, England, 1987; Vol. 3, p 1023. (c) Pope, M. T.; Müller, A. *Angew. Chem., Int. Ed. Engl.* **1991**, *30*, 29.
(2) Tytko, K.-H.; Glemser, O. *Adv. Inorg. Chem. Radiochem.* **1976**, *19*, 239.
(3) Weakly, T. J. R. *Struct. Bonding (Berlin)* **1974**, *18*, 131. Tsigdinos, P. A. *Top. Curr. Chem.* **1978**, *76*, 1.
(4) Day, V. W.; Klemperer, W. G. *Science* **1985**, *228*, 533.
(5) Chen, Q.; Zubieta, J. *Coord. Chem. Rev.* **1992**, *114*, 107, and references therein.
(6) Jeannin, Y.; Hervé, G.; Proust, A. *Inorg. Chem. Acta* **1992**, *198–200*, 319.
(7) Adams, R. D.; Klemperer, W. G.; Liu, R.-S. *J. Chem. Soc., Chem. Commun.* **1979**, 256.
(8) McCarron, E. M., III; Harlow, R. C. *J. Am. Chem. Soc.* **1983**, *105*, 6179.
(9) Day, V. W.; Thompson, M. R.; Klemperer, W. G.; Liu, R.-S. *J. Am. Chem. Soc.* **1980**, *102*, 5971.
(10) Chen, Q.; Liu, S.; Zhu, H.; Zubieta, J. *Polyhedron* **1989**, *8*, 2915.
(11) Zubieta, J. *Proceedings of the Workshop on Polyoxoanions: Polyoxometalates: From Platonic Solids to Anti-retroviral Activity*; Bielefeld, Germany, 1992.
(12) Day, V. W.; Fredrich, M. F.; Klemperer, W. G.; Shum, W. *J. Am. Chem. Soc.* **1977**, *99*, 6146.
(13) Fuchs, J.; Hartl, H. *Angew. Chem., Int. Ed. Engl.* **1976**, *15*, 375. Klemperer, W. G.; Shum, W. *J. Am. Chem. Soc.* **1976**, *98*, 8291.
(14) Day, V. W.; Klemperer, W. G.; Yaghi, O. M. *J. Am. Chem. Soc.* **1989**, *111*, 4518.
(15) Day, V. W.; Klemperer, W. G.; Maitlis, D. J. *J. Am. Chem. Soc.* **1987**, *109*, 2991.
(16) McCarron, E. M., III; Whitney, J. F.; Chase, D. O. *Inorg. Chem.* **1984**, *23*, 3276.
(17) Hsieh, T.-C.; Zubieta, J. *Inorg. Chem.* **1985**, *24*, 1287. (b) Hsieh, T.-C.; Zubieta, J. *Polyhedron* **1985**, *5*, 309. (c) Hsieh, T.-C.; Zubieta, J. *Polyhedron* **1985**, *5*, 1655. (d) Shaikh, S. N.; Zubieta, J. *Inorg. Chem.* **1986**, *25*, 4613. (e) Hsieh, T.-C.; Zubieta, J. *J. Chem. Soc. Chem. Commun.* **1985**, 1749. (f) Hseih, T.-C.; Shaikh, S. N.; Zubieta, J. *Inorg. Chem.* **1987**, *26*, 4079. (g) Shaikh, S. N.; Zubieta, J. *Inorg. Chim. Acta* **1986**, *121*, 243. (h) Liu, S.; Zubieta, J. *Polyhedron* **1988**, *7*, 401. (i) Chen, Q.; Liu, S.; Zubieta, J. *Inorg. Chim. Acta* **1989**, *164*, 115.
(18) Kang, H.; Liu, S.; Shaikh, S. N.; Nicholson, T.; Zubieta, J. *Inorg. Chem.* **1989**, *28*, 920.
(19) Bradley, D. C.; Mehrotra, R. C.; Gaur, D. P. *Metal Alkoxides*; Academic Press: New York, 1978.

0020-1669/93/1332-2929$04.00/0

oxide coordination compounds and molecular species which serve as a bridge between the oligomeric metal alkoxides $[M(OR)_n]_x$ and the macromolecular metal oxides,[20,25] relatively few structurally characterized examples have been described. Structural prototypes for this cluster subclass are represented by $[Ti_7O_4(OEt)_{20}]$[26] and $[Nb_8O_{10}(OEt)_{20}]$,[27] species which exhibit close structural affinities to the polyoxoanion clusters $[Mo_7O_{24}]^{6-}$[28] and $[H_2W_{12}O_{42}]^{10-}$,[29] respectively. In addition to such fully oxidized (d^0) metal cores, polyoxoalkoxy transition metal clusters with reduced or mixed-valence metal centers provide a recurrent theme of the structural chemistry of polyoxoalkoxometalate species. Examples include the Mo(IV) species $[Mo_4O_8(OR)_4(pyridine)_4]^{4-}$,[30] the Mo(V) cluster $[Mo_4O_8(OR)_2(HOR)_2Cl_4]^{2-}$,[31] and the mixed-valence complexes $[Mo_6O_{10}(OR)_{12}]$[32] and $[Mg_2Mo_8O_{22}(OR)_6(HOR)_4]^{2-}$.[33]

Our investigations have focused on the use of polyalkoxide ligands as structural buttresses in the synthesis of novel cluster types. The tris(hydroxymethyl)alkane class of ligands, $(HOCH_2)_3CR$ or (H_3tris), has proved particularly effective in this regard as a consequence of the ligand steric constraints which favor the adoption of a bridging coordination mode about a triangular metal core (structure I). This fundamental structural motif is present

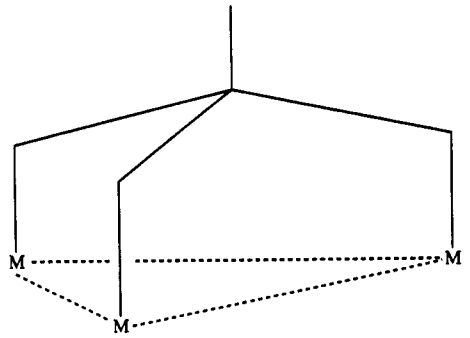

I

in the polyoxomolybdate clusters $[Mo_3O_7(tris)_2]^{2-}$,[34] $[Mo_4O_8(OR)_2(tris)_2]$,[35] and $[H_2Mo_8O_{20}(OR)_4(tris)_2]$[36] and in the extensive series of polyoxovanadates of the general type $[V_6O_{13-n}(OH)_n(tris)_2]^{2-}$, n = 0, 2, 3, 4 and 6.[37]

More recently, we have sought to extend the chemistry of polyoxoalkoxometalate clusters by exploiting the techniques of hydrothermal synthesis.[38-41] Under the conditions of temperatures in the 120–220 °C range at autogenous pressure which we have employed, a variety of polyoxometalate clusters incorporating common organic ligands have been isolated and structurally characterized. These include polyoxoalkoxovanadium clusters adopting hexavanadate $\{V_6O_{19}\}$ and decavanadate $\{V_{10}O_{28}\}$ core geometries[38,39] and supramolecular clusters of which $[Na(H_2O)_3H_{15}Mo_{42}O_{109}(tris)_7]^{7-}$[40] is prototypical. Both vanadium cores, shown in structure II, illustrate the preferred substitution

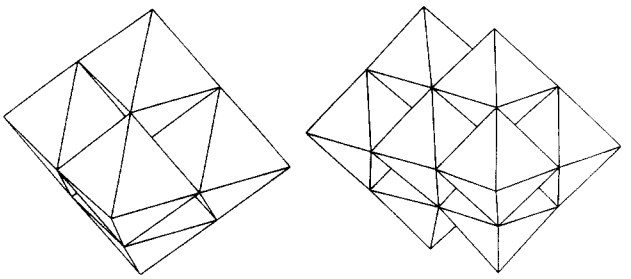

II

pattern adopted by the trialkoxy ligand types, reflecting the geometric constraints of the ligand which favor a coordination mode bridging a triangular arrangement of metal sites. Thus, in both cluster types, the ligands cap the triangular faces of the tetrahedral cavities of the fused polyhedral framework.

In this paper, we describe the hydrothermal synthesis and structural and chemical characterization of a series of reduced and mixed valence clusters possessing the hexametalate core geometry: $Ba[V_6O_7(OH)_3\{(OCH_2)_3CCH_3\}_3]\cdot 3H_2O$ (**1**), $Na_2[V_6O_7\{(OCH_2)_3CCH_2CH_3\}_4]$ (**2**), $(Me_3NH)[V_6O_7(OH)_3\{(OCH_2)_3CCH_3\}_3]$ (**3**), and $Na[V_6O_6F(OH)_3\{(OCH_2)_3CCH_3\}_3]\cdot 3H_2O$ (**4**). Cluster **4** is a unique example of fluoride substitution for the central oxo group of a hexametalate core, an observatioin consistent with the pronounced tendency of polyvanadate hosts to encapsulate a variety of chemical species.[42]

Experimental Section

Reagent grade chemicals were used throughout. Vanadium(III) oxide (Aldrich), vanadium(V) oxide (Aldrich), ammonium metavanadate (Alfa), 1,1,1-tris(hydroxymethyl)ethane (Aldrich), 1,1,1-tris(hydroxymethyl)propane (Fluka), trimethylamine (Aldrich), and ammonium chloridie were used as received from the commercial sources.

Preparation of $Ba[V_6O_7(OH)_3\{(OCH_2)_3CCH_3\}_3]\cdot 3H_2O$ (1). After V_2O_3, KVO_3, 1,1,1-tris(hydroxymethyl)ethane, $BaCl_2\cdot 2H_2O$, and H_2O were mixed in the mole ratio 3:6:10:10:300, the reaction mixture was placed in a Teflon-lined autoclave and heated for 50 h at 150 °C at autogenous pressure. After the contents of the autoclave were cooled to room temperature, light blue crystals of **1** were filtered from the colorless mother liquor, washed with water, and air dried (yield: 30%). Anal. Calcd for $C_{15}H_{36}BaO_{22}V_6$: C, 17.8; H, 3.56. Found: C, 18.4; H, 3.91. IR (KBr pellet, cm^{-1}): 1457 (w), 1260 (m), 1115 (s), 1050 (vs), 981 (s), 946 (s), 899 (w), 803 (m), 603 (s), 571 (s), 486 (s).

The Rb analogue, $Rb_2[V_6O_7(OH)_3\{(OCH_2)_3CCH_3\}_3]$ (**1a**) was prepared in a similar fashion (yield: 40%). IR (KBr pellet, cm^{-1}): 1462 (w), 1407 (w), 1213 (w), 1130 (s), 1047 (vs), 972 (s), 941 (s), 929 (s), 822 (m), 799 (m), 611 (s), 567 (vs), 484 (s).

Preparation of $Na_2[V_6O_7\{(OCH_2)_3CCH_2CH_3\}_4]$ (2). A mixture of V_2O_3, $NaVO_3$, 1,1,1-tris(hydroxymethyl)propane, NaCl, and H_2O in the mole ratio 3:6:10:5:300 was heated for 21 h at 150 °C in a Teflon-

(20) Mehrotra, R. C. Transition Metal Alkoxides. In *Advances in Inorganic Radiochemistry*; Emeleus, H. G., Sharpe, A. G., Eds.; Academic Press: New York, 1983; Vol. 26, p 269.
(21) Chisholm, M. H. In *Chemistry Toward the 21st Century*; American Chemical Society: Washington, DC, 1983; p 243.
(22) Chisholm, M. H. In *Comprehensive Coordination Chemistry*; Wilkinson, G., McCleverty, J. A., Eds.; Pergamon Press: Oxford, England, 1987.
(23) Bradley, P. C. *Chem. Rev.* **1989**, *89*, 1317.
(24) Caulton, K. G.; Hubert-Pfalzgraf, J. G. *Chem. Rev.* **1990**, *90*, 969.
(25) Misono, M. *Catal. Rev.—Sci. Eng.* **1987**, *29*, 269.
(26) Day, V. W.; Eberspacher, T. A.; Klemperer, W. G.; Park, C. W.; Rosenburg, F. S. *J. Am. Chem. Soc.* **1991**, *113*, 8190. (b) Watenpaugh, K.; Cauglan, C. N. *J. Chem. Soc., Chem. Commun.* **1967**, 76.
(27) Bradley, D. C.; Hursthouse, M. B.; Rodesila, P. F. *J. Chem. Soc., Chem. Commun.* **1968**, 1112.
(28) Kepert, D. L. *The Early Transition Metals*; Academic Press: London, 1972.
(29) Keggin, J. F. *Nature* **1933**, *131*, 908.
(30) Chisholm, M. H.; Huffman, J. C.; Kirkpatrick, C. C.; Leonelli, J.; Folting, K. *J. Am. Chem. Soc.* **1981**, *103*, 6093.
(31) Kang, H.; Liu, S.; Shaikh, S. N.; Nicholson, T.; Zubieta, J. *Inorg. Chem.* **1989**, *28*, 920.
(32) Chisholm, M. H.; Folting, K.; Huffman, J. C.; Kirkpatrick, C. C. *Inorg. Chem.* **1984**, *23*, 1021.
(33) Yu Antipis, M.; Didenko, L. P.; Kachapina, L. M.; Shilov, A. E.; Shilova, A. K.; Struchkov, Y. T. *J. Chem. Soc., Chem. Commun.* **1989**, 1467.
(34) (a) Ma, L.; Liu, S.; Zubieta, J. *Inorg. Chem.* **1989**, *28*, 175; (b) Gumaer, E.; Lettko, K.; Ma, L.; Macherone, D.; Zubieta, J. *Inorg. Chem. Acta* **1991**, *179*, 47. (c) Liu, S.; Ma, L.; McGowty, D.; Zubieta, J. *Polyhedron* **1990**, *9*, 1541.
(35) (a) Knobler, C. B.; Penfold, B. R.; Robinson, W. T.; Wilkins, C. J.; Yong, S. M. *J. Chem. Soc., Dalton Trans.* **1980**, 284. (b) Wilson, A. J.; Robinson, W. T.; Wilkins, C. J. *Acta Crystallogr.* **1983**, *C39*, 54.
(36) Ma, L.; Liu, S.; Zubieta, J. *J. Chem. Soc., Chem. Commun.* **1989**, 440.
(37) Chen, Q.; Goshorn, D. P.; Scholes, C. P.; Tan, X.-L.; Zubieta, J. *J. Am. Chem. Soc.* **1992**, *114*, 4667.
(38) Khan, M. I.; Chen, Q.; Zubieta, J. *Inorg. Chem.* **1992**, *31*, 1556.
(39) Khan, M. I.; Chen, Q.; Goshorn, D. P.; Hope, M.; Parkin, S.; Zubieta, J. *J. Am. Chem. Soc.* **1992**, *114*, 3341.
(40) Khan, M. I.; Zubieta, J. *J. Am. Chem. Soc.* **1992**, *114*, 10058.
(41) For general references on the technique see: (a) Figlarz, M. *Chim. Scr.* **1988**, *28*, 3. (b) Rouxel, J. *Chim. Scr.* **1988**, *28*, 33. (c) Livage, J. *Chim. Scr.* **1988**, *28*, 9.
(42) Klemperer, W. G.; Marquart, T. A.; Yaghi, O. M. *Angew. Chem., Int. Ed. Engl.* **1992**, *31*, 49.

Table I. Crystallographic Data for the Structural Studies of $Ba[V_6O_7(OH)_3\{(OCH_2)_3CCH_3\}_3]\cdot 3H_2O$ (1), $Na_2[V_6O_7\{(OCH_2)_3CCH_2CH_3\}_4]$ (2), $(Me_3NH)[V_6O_7(OH)_3\{(OCH_2)_3CCH_3\}_3]$ (3), and $Na[V_6O_6F(OH)_3\{(OCH_2)_3CCH_3\}_3\cdot 3H_2O$ (4)

	1	2	3	4
chem formula	$C_{15}H_{36}BaO_{22}V_6$	$C_{24}H_{44}O_{19}V_6Na_2$	$C_{18}H_{40}NO_{19}V_6$	$C_{15}H_{36}FNaO_{21}V_6$
fw	1011.4	988.2	880.1	901.1
T, °C	153	296	296	153
λ, Å	1.541 78	0.710 73	0.710 73	1.541 78
a, Å	13.707(1)	19.202(4)	12.792(3)	12.977(1)
c, Å	9.647(2)		10.692(2)	10.160(1)
V, Å^3	1569.7(2)	7080(1)	1515.2(6)	1481.7(2)
space group	$P6_3mc$	$Fd3$	$P6_3mc$	$P6_3mc$
Z	2	8	2	2
D_{calc}, g cm^{-3}	2.140	1.854	1.929	2.020
μ, cm^{-1}	247.2	15.7	17.9	164.7
R^a	0.0576	0.0509	0.0410	0.0371
R_w^b	0.0669	0.0712	0.0462	0.0403

^{a} $R = \sum||F_o| - |F_c||/\sum|F_o|$. ^{b} $R_w = [\sum w(|F_o| - |F_c|)^2/\sum w(F_o)^2]^{1/2}$.

lined autoclave. After the reaction vessel was cooled to room temperature over a 4-h period, sky blue crystals of **2** were filtered, mechanically separated from a dark amorphous material and air dried (yield: 70%). Anal. Calcd for $C_{24}H_{44}O_{19}V_6Na_2$: C, 29.2; H, 4.49. Found: C, 29.0; H, 4.25. IR (KBr pellet, cm^{-1}): 1466 (m), 1447 (m), 1403 (m), 1203 (m), 1115 (vs), 1046 (vs), 983 (sh), 951 (vs, broad), 770 (w), 602 (s), 578 (vs), 490 (s).

Preparation of $(Me_3NH)[V_6O_7(OH)_3\{(OCH_2)_3CCH_3\}_3]$ (3). A mixture of V_2O_3, V_2O_5, 1,1,1-tris(hydroxymethyl)ethane, Me_3NHCl, Et_3NHCl, and H_2O in the mole ratio 1.25:1.25:2.5:5:5:300 was heated for 17 h at 210 °C. After this mixture was cooled to room temperature over a period of 3 h, light yellow-green needles of **3** were filtered from the mother liquor and air driied (yield: 30%). IR (KBr pellet, cm^{-1}): 1460 (m), 1397 (m), 1209 (w), 1136 (s), 1044 (vs), 978 (s), 949 (s), 932 (s), 615 (s), 574 (vs), 487 (s).

Preparation of $Na[V_6O_6(OH)_3F\{(OCH_2)_3CCH_3\}_3]\cdot 3H_2O$ (4). A mixture of V_2O_3, $NaVO_3$, 1,1,1-tris(hydroxymethyl)ethane, $NaBF_4$, NaCl, and H_2O in the mole ratio 2.5:5:10:10:5:300 was heated for 24 h at 150 °C. After the reaction was cooled to room temperature over a period of 6 h, long green needles of **4** were collected by filtration and air dried (yield: 60%). Anal. Calcd for $C_{15}H_{33}O_{21}FNaV_6$: C, 20.1; H, 3.68; F, 2.12. Found: C, 19.6; H, 3.43; F, 2.01. IR (KBr pellet, cm^{-1}): 1612 (s), 1458 (m), 1400 (m), 1214 (m), 1127 (s), 1046 (sh), 1024 (vs), 1002 (s), 987 (s), 920 (w), 611 (s), 570 (vs), 485 (s).

X-ray Crystallographic Studies. Compounds **2** and **3** were studied using a Rigaku APC5S diffractometer. However, compounds **1** and **4** crystallized as thin needles, and data of sufficient qualiity for structure refinement could not be obtained using a conventional sealed tube instrument. Consequently, data were collected on a Siemens P3RA rotating anode diffractometer at 120 K. The crystal parameters and experimental conditions for data collection are summarized in Table I. A complete description of the crystallographic methods is given in the supplementary materials. Since the Rb analogue **1a** is isomorphous to the Ba derivative **1**, no further structural work beyond refinement of the unit cell parameters was performed. Crystal data for **1a**: hexagonal space group $P6_3mc$, a = 13.008(2) Å, c = 9.958(3) Å, V = 1459.2(4) Å^3.

The structures were solved by Patterson methods and refined by full-matrix least-squares methods using the SHELXTL program package. The details of the structure solutions and refinements are presented in the supplementary materials. No anomalies were encountered in the solutions of these structures. Atomic positional parameters and isotropic temperature factors for **1–4** are presented in Tables II–V, respectively. Bond lengths and angles for **1–4** are presented in Tables VI–IX, respectively.

Magnetism. The magnetic susceptibility data were recorded on a 15.5 mg polycrystalline sample of $Rb_2[V_6O_7(OH)_3\{(OCH_2)_3CCH_3\}_3]$ over the 6–200 K temperature region using a SQUID susceptometer. Measurement and calibration techniques have been reported elsewhere.[60] The magnetic data are shown in Figure 8 as molar magnetic susceptibility plotted as a function of temperature over the 6–200 K temperature region. The data for complexes **2** and **3** was collected over a temperature range of 5–300 K in an applied filler of 6 kG using a Quantum Design Model MPMS SQUID Magnetmeter. Magnetization isotherms at 298 and 77 K were performed to correct for the presence of ferromagnetic impurities.

Electrochemical Studies. Cyclic voltammetric studies and controlled potential electrolyses for complex **4** were carried out in an acetonitrile solution 1.0 × 10^{-3} M in complex and 0.1 M in $(n\text{-}C_4H_9)_4NPF_6$ as supporting electrolyte. Platinum-bead and platinum-mesh working electrodes were used in the cyclic voltatammetry and controlled-potential electrolysis, respectively. All potentials are referenced to Ag/AgCl.

In the case of **2**, cyclic voltammetry was carried out in a H_2O solution 1.0 × 10^{-3} M in complex and 0.1 M in $NaClO_4$ and 0.01 M in $HClO_4$ as supporting electrolyte, using a polished, glassy-carbon electrode. Controlled-potential electrolyses were conducted at a stirred mercury pool electrode.

Table II. Atomic Coordinates (×10^4) and Equivalent Isotropic Displacement Coefficients (Å^2 × 10^3) for 1

	x	y	z	U(eq)^a
V(1)	4110(2)	5890(2)	2436	20(1)
V(2)	2530(2)	5060(3)	5199(7)	23(1)
Ba	3333	6667	8641(6)	15(1)
O(1)	3333	6667	3814(32)	7(6)
O(2)	1300(9)	4605(8)	3883(14)	29(3)
O(3)	2662(7)	5323(13)	1461(22)	27(4)
O(4)	3994(6)	6006(6)	6177(19)	22(3)
O(5)	1994(9)	3987(19)	6314(27)	54(5)
O(6)	4705(7)	5295(7)	1669(20)	40(5)
O(7)	4457(7)	5543(7)	8954(19)	52(9)
C(1)	818(16)	3503(15)	3290(20)	40(6)
C(2)	1683(12)	3365(24)	2440(43)	56(9)
C(3)	2061(13)	4122(26)	1170(36)	42(7)
C(4)	1325(21)	2052(25)	1925(33)	22(8)

^{a} Equivalent Isotropic U defined as one-third of the trace of the orthogonalized U_{ij} tensor.

Table III. Atomic Positional Parameters (×10^4) and Isotropic Displacement Coefficients (Å^2 × 10^3) for 2

atom	x	y	z	U(eq)^a
V	0.00443(8)	1/8	1/8	20.6(9)
Na	0	0	0	22.47(2)
O(1)	1/8	1/8	1/8	19(3)
O(2)	0.0219(2)	0.1233(2)	0.0222(3)	20.8(9)
O(3)	–0.0786(4)	1/8	1/8	24(1)
C(1)	–0.0163(7)	0.1734(5)	–0.0180(6)	26(2)
C(2)	0.2494(6)	0.2494	0.2494	31(4)
C(3)	0.2977(7)	0.2977	0.2977	26(5)
C(4)	–0.0333	0.3821	–0.0286	30(10)

^{a} Equivalent isotropic U defined as one-third of the trace of the orthogonalized U_{ij} tensor.

Results and Discussion

Synthesis and Electrochemistry. While the techniques of hydrothermal synthesis have been employed extensively in geochemistry and industrial crystal growth,[43,44] routine exploitation in conventional inorganic synthesis is a relatively recent development.[45–47] Hydrothermal synthesis is an example of

(43) Laudise, R. A. *Chem. Eng. News* **1987**, Sept. 28, 30.
(44) Lobachev, A. N.; Archand, G. D. *Crystallization Processes under Hydrothermal Conditions*; Consultants Bureau: New York, 1973.

Table IV. Atomic Positional Parameters (×10⁴) and Isotropic Displacement Coefficients (Å² × 10³) for **3**

atom	x	y	z	U(eq)[a]
V(1)	0.58249(6)	1.1650	1/2	13.6(5)
V(2)	0.4934(1)	0.2467	0.7473(2)	15.9(7)
O(1)	0.6667	0.3333	0.615(1)	15(1)
O(2)	0.5942(3)	1.1884	0.8266(7)	18(1)
O(3)	0.5222(5)	0.2611	0.4089	15(2)
O(4)	0.4465	0.1170	0.6222	16(1)
O(5)	0.5226	1.0452	0.4151	18(2)
O(6)	0.3765	0.1882	0.8351	23(4)
N(1)	0.6667	0.3333	1.115(1)	32(3)
C(1)	0.8013(4)	−0.8013	0.378(1)	17(1)
C(2)	0.3283(6)	1.0654(5)	0.5688(6)	18(2)
C(3)	0.8435(4)	−0.8435	0.489(1)	17(1)
C(4)	0.1830	0.0915	0.437(12)	23(7)
C(6)	0.6039(8)	1.2079	1.122(2)	32(10)

[a] Equivalent isotropic U defined as one-third of the trace of the orthogonalized U_{ij} tensor.

Table V. Atomic Coordinates (×10⁴) and Equivalent Isotropic Displacement Coefficients (Å² × 10³) for **4**

	x	y	z	U(eq)[a]
V(1)	4188(1)	5812(1)	2500	11(1)
V(2)	15089(1)	7545(1)	−189(3)	14(1)
F(1)	3333	6667	1357(11)	18(2)
O(1)	4760(2)	5240(2)	3494(7)	15(1)
O(2)	2632(2)	5264(4)	3486(8)	12(1)
O(3)	5479(3)	6684(3)	1243(6)	13(1)
O(4)	16237(5)	8118(3)	−1034(8)	25(2)
O(5)	4035(2)	8071(5)	−881(8)	18(2)
C(1)	692(5)	3338(5)	1797(7)	17(1)
C(2)	1993(3)	3985(6)	3843(10)	14(2)
C(3)	1582(3)	3164(7)	2626(10)	17(2)
C(4)	943(4)	1886(8)	3163(12)	24(2)
Na	3333	6667	5288	20(2)
O(6)	4238(3)	8476(6)	6258(12)	40(2)

[a] Equivalent isotropic U defined as one-third of the trace of the orthogonalized U_{ij} tensor.

Table VI. Selected Bond Lengths (Å) and Angles (deg) for **1**

V(1)–O(1)	2.272(18)	V(1)–O(3)	1.971(11)
V(1)–O(6)	1.596(9)	V(2)–O(1)	2.328(19)
V(1)–O(2B)	2.079(12)	V(2)–O(4)	1.999(12)
V(2)–O(2)	1.947(13)	Ba–O(4)	2.848(16)
V(2)–O(5)	1.667(24)	Ba–O(3A)	3.154(20)
Ba–O(7)	2.685(2)		
Ba–O(4A)	2.848(17)		
Ba–O(7A)	2.685(8)		
O(1)–V(1)–O(3)	81.3(6)	O(1)–V(1)–O(6)	171.8(9)
O(3)–V(1)–O(6)	104.4(7)	O(1)–V(1)–O(2A)	80.2(6)
O(3)–V(1)–O(2A)	161.5(6)	O(6)–V(1)–O(2A)	93.9(6)
O(2)–V(2)–O(4)	160.6(5)	O(1)–V(2)–O(2)	81.6(6)
O(1)–V(2)–O(5)	174.8(11)	O(1)–V(2)–O(4)	79.1(6)
O(4)–V(2)–O(5)	97.1(8)	O(2)–V(2)–O(5)	102.0(7)
V(2A)–O(1)–V(2B)	90.4(9)	V(2)–O(2)–C(1)	117.9(13)
V(2)–O(2)–V(1B)	108.0(4)	C(1)–O(2)–V(1B)	114.2(11)
V(1)–O(3)–C(3)	115.3(8)	V(1)–O(3)–V(1B)	108.1(9)
C(3)–O(3)–BaA	109.2(17)	V(1)–O(3)–BaA	103.8(5)
V(1)–O(1)–V(2)	90.2(1)	V(1B)–O(3)–BaA	103.8(5)
V(2)–O(1)–V(1A)	179.2(3)	V(2)–O(4)–V(2A)	111.4(8)
		V(1)–O(1)–V(1A)	89.2(9)

"chimiei douce" or "soft chemistry", which employs temperatures ranging from ambient to 300 °C and autogenous pressures.[41]

Hydrothermal syntheses are conventionally carried out in water at 150–250 °C at autogenous pressure. The lower viscosity of water under these conditions results in enhanced rates of solvent extraction of solids and crystal growth from solution.[43] Since

Table VII. Selected Bond Lengths (Å) and Angles (deg) for **2**

V–O(1)	2.315(2)	O(2)–C(1)	1.43(1)
V–O(2)	2.003(5)	C(1)–C(2)	1.54(1)
V–O(2)	2.010(5)	C(2)–C(3)	1.60(3)
V–O(3)	1.593(7)	C(3)–C(4)	1.685(8)
O(1)–V–O(2)	80.4(1)	O(2)–C(1)–C(2)	114(1)
O(1)–V–O(3)	180.00	C(1)–C(2)–C(3)	107.0(8)
O(2)–V–O(3)	99.6(1)	C(2)–C(3)–C(4)	109.6(8)
V–O(2)–C(1)	115.7(5)		

Table VIII. Selected Bond Lengths (Å) and Angles (deg) for **3**

V(1)–O(1)	2.236(7)	O(3)–C(1)	1.42(1)
V(1)–O(3)	2.001(4)	O(4)–C(2)	1.432(7)
V(1)–O(4)	2.010(4)	N(1)–C(6)	1.39(2)
V(1)–O(5)	1.608(7)	C(2)–C(3)	1.534(9)
V(2)–O(1)	2.382(8)	C(3)–C(4)	1.54(1)
V(2)–O(2)	1.974(4)		
V(2)–O(4)	1.976(4)		
V(2)–O(6)	1.600(7)		
O(1)–V(1)–O(3)	79.9(2)	V(1)–O(3)–C(1)	116.0(3)
O(1)–V(1)–O(4)	82.1(2)	V(1)–O(4)–V(2)	109.3(2)
O(1)–V(1)–O(5)	179.1(4)	V(1)–O(4)–C(2)	115.7(4)
O(3)–V(1)–O(4)	87.9(2)	V(2)–O(4)–C(2)	117.7(4)
O(3)–V(1)–O(5)	99.5(2)	O(3)–C(1)–C(3)	114.5(8)
O(1)–V(2)–O(2)	78.4(2)	O(4)–C(2)–C(3)	112.2(5)
O(1)–V(2)–O(4)	79.1(2)	C(1)–C(3)–C(2)	111.6(5)
O(2)–V(2)–O(4)	87.4(3)	C(1)–C(3)–C(4)	107.1(9)
O(2)–V(2)–O(6)	101.9(3)	C(2)–C(3)–C(4)	107.6(5)
V(1)–O(1)–V(2)	89.49(4)		

Table IX. Selected Bond Lengths (Å) and Angles (deg) for **4**

V(1)–F(1)	2.245(6)	V(1)–O(1)	1.634(4)
V(1)–O(2)	2.037(4)	V(1)–O(3)	1.955(5)
V(2)–O(3A)	2.045(6)	V(1)–O(2A)	2.037(5)
V(2)–O(5A)	1.940(4)	V(2)–O(4)	1.549(7)
O(2)–C(2)	1.482(9)	O(2)–Na	2.416(9)
C(1)–O(3B)	1.448(7)	C(1)–C(3)	1.534(9)
C(3)–C(4)	1.536(12)	C(2)–C(3)	1.543(13)
Na–O(6)	2.260(9)		
F(1)–V(1)–O(1)	173.0(3)	F(1)–V(1)–O(2)	77.2(2)
O(1)–V(1)–O(2)	97.7(2)	F(1)–V(1)–O(3)	82.4(2)
O(1)–V(1)–O(3)	102.4(2)	O(2)–V(1)–O(3)	159.4(2)
O(2)–V(1)–O(2A)	84.1(3)	O(1)–V(1)–O(2A)	97.7(3)
O(1)–V(1)–O(3C)	102.4(2)	O(3)–V(1)–O(2A)	88.5(2)
O(3)–V(1)–O(3C)	91.8(3)	O(3A)–V(2)–O(5A)	149.3(3)
O(2A)–V(1)–O(3C)	159.4(3)		
O(4)–V(2)–O(3D)	102.5(2)		
O(4)–V(2)–O(5A)	107.9(3)		
O(3D)–V(2)–O(5A)	85.2(2)		
O(5A)–V(2)–O(5B)	89.5(2)		
V(1)–F(1)–V(1B)	95.7(3)		

differential solubility problems are minimized, a variety of synthetic precursors may be introduced. An additional advantage is that a variety of templating cations, including organic cations, may be employed, and during the crystallization process, the templates of appropriate size or geometry to fill the crystal vacancies are "selected" from the mixture. The technique exploits the principle of "self assembly" of the metastable solid phase from soluble precursors at relatively low temperatures.

While rational design of a desired product by hydrothermal techniques remains an elusive goal, the vast parameter space of stoichiometries, cation identity, pH, fill volume, temperature, heating time, and so on may be manipulated to obtain a variety of metastable species not otherwise accessible by conventional synthetic techniques. Thus, in the presence of Ba^{2+}, vanadate and $(HOCH_2)_3CCH_3$ react to give the fully reduced hexametalate species $Ba[V_6O_7(OH)_3\{(OCH_2)_3CCH_3\}_3]\cdot 3H_2O$ (**1**) where nine oxo groups of the hypothetical $\{V_6O_{19}\}$ core have been replaced by bridging alkoxy donors. In contrast, when Na^+ is used as template and $(HOCH_2)_3CCH_2CH_3$ as ligand, $Na_2[V_6O_7\{(OCH_2)_3CCH_2CH_3\}_4]$ (**2**) is isolated, a species in which all 12 doubly bridging oxo groups of the parent core have been

(45) Haushalter, R. C.; Mundi, L. A. *Chem. Mater.* **1992**, *4*, 31 and references therein.
(46) Huan, G.; Day, V. W.; Jacobson, A. J.; Goshorn, D. P. *J. Am. Chem. Soc.* **1991**, *113*, 3188 and reference therein.
(47) Liao, J. H.; Kanatzidis, M. G. *Inorg. Chem.* **1992**, *31*, 431.

Table X. Voltammetric Parameters for the Pedox Processes of 2 and 4

compound	$E_{1/2}$, V[c]	$E_p^f - E_p^r$, mV	i_p^f/i_p^r	$i_p/Cv^{1/2}$, mA $s^{1/2}$ $mV^{-1/2}$ M^{-1} [d]	n_{app}[e]
$Na_2[V_6O_7\{(OCH_2)_3CCH_2CH_3\}_4]$[a]	+0.21	65	1.0	9.1	1.0
	+0.47	72	1.0	9.2	1.0
$Na[V_6O_6F(OH)_3\{(OCH_2)_3CCH_3\}_3]\cdot 3H_2O$[b]	+0.34	64	1.0	12.3	1.0
	+0.49	71	1.0	11.9	1.0

[a] At a platinum working electrode, using solutions 1.0×10^{-3} M in complex and 0.1 M in $(TBA)PF_6$ in acetonitrile. [b] At a glassy-carbon election, using solutions 1.0×10^{-3} M in complex and 0.1 M $NaClO_4$/0.01 M $HClO_4$ in water. [c] All potentials are referenced to Ag/AgCl. Cyclic voltammograms were obtained at sweep rates of 200 mV s^{-1}. $E_{1/2}$ is estimated from the expression $E_{1/2} = (E_p^f - E_p^r)/2 \sim E_p^f - 29$ mV. The shape parameter for $E_p^f - E_p^r$ lay within the range 60–75 mV for all couples. [d] The current function for ferrocene/ferrocenium couple at the Pt electrode is 9.2 mA $s^{1/2}$ $mV^{-1/2}$ M^{-1}, while it is 12.2 mA $s^{1/2}$ $mV^{-1/2}$ M^{-1} at the glassy-carbon electrode. [e] The value of n (number of electrons) was determined by controlled-potential electrolysis.

replaced by bridging alkoxy groups. The introduction of an organic template Me_3NH^+ results in the isolation of $(Me_3NH)[V_6O_7(OH)_3\{(OCH_2)_3CCH\}_3]$ (**3**), a mixed-valence V(IV)/V(V) species which exhibits gross structural features similar to those of **1**. The influence of mineralizing reagents is most dramatically illustrated by the reaction of vanadate and $(HOCH_2)_3CCH_3$ in the presence of $NaBF_4$ which results in incorporation of F^- as a hostage anion in the hexavanadium framework of $Na[V_6O_6F(OH)_3\{(OCH_2)_3CCH_3\}_3]\cdot 3H_2O$ (**4**).

While compounds **1** and **3** are totally insoluble in water and common polar organic solvents, compound **4** was readily soluble in acetonitrile, giving a bright blue solution. In contrast, compound **2** was solubilized in H_2O over a 48 h period with vigorous stirring. Solutions of **2** and **4** are unstable in the presence of oxygen, decomposing to give light yellow solutions. Degassed solutions of **2** and **4** are stable for a period of several days.

The cyclic voltammogram of **4** at a platinum-bead electrode in 0.1 M $(TBA)PF_6$ in acetonitrile exhibits successive reversible one-electron oxidations at +0.34 and +0.49 V with respect to Ag/AgCl. The processes are judged electrochemically reversible on the bases of the ratio of peak heights for the anodic and cathodic processes and the peak-to-peak separations (Table X). The electrochemical parameters of **4** are consistent with the following processes:

$$[V_6O_6F(OH)_3\{(OCH_2)_3CCH_3\}_3]^+ \overset{+0.49}{\rightleftharpoons} [V_6O_6F(OH)_3\{(OCH_2)_3CCH\}_3] \overset{+0.34}{\rightleftharpoons} [V_6O_6F(OH)_3\{(OCH_2)_3CCH_3\}_3]^-$$

The cyclic voltammetry of **2** at a glassy carbon electrode in 0.1 M $NaClO_4$ in water likewise exhibits two successive one-electron oxidations, at potentials of +0.21 and +0.47 V. Although the peak height ratio for these processes is 1.0 for various sweep rates, the peak-to-peak separation ΔE_p increases with increasing sweep rate, consistent with quasi-reversible processes characterized by slow electron transfer:

$$[V_6O_7\{(OCH_2)_3CCH_2CH_3\}_4]^0 \overset{+0.47}{\rightleftharpoons} [V_6O_7\{(OCH_2)_3CCH_2CH_3\}_4]^- \overset{+021}{\rightleftharpoons} [V_6O_7\{(OCH_2)_3CCH_2CH_3\}_4]^{2-}$$

While the different conditions employed in the cyclic voltammetry of **2** and **4** allow only gross comparisons of the electrochemical characteristics, the relative ease of the first oxidation process for **2** may reflect the difference in cluster charges: the dinegative anion of **2** is more easily oxidized than the mononegative anion of **4**.

As anticipated, the electrochemistry of **2** and **4**, which is characterized by anodic processes, contrasts with that of the $[V_6O_{13}\{(OCH_2)_3CR\}_2]^{2-}$ series of clusters[37] which exhibit cathodic processes at moderately negative potentials. This observation reflects the presence of reduced V(IV) sites in **2** and **4** and oxidized V(V) centers in the $[V_6O_{13}\{(OCH_2)_3CR\}_2]^{2-}$ series. Clusters of the related series with reduced centers, such as $[V_6O_7(OH)_6\{(OCH_2)_3CR\}_2]^{2-}$, are oxidized much more readily, exhibiting successive one-electron oxidations at –0.45 and –1.22 V with respect to Ag/AgCl. Apparently, the introduction of additional trialkoxy ligands about the hexavanadium core makes the cluster considerably more difficult to oxidize. This is consistent with the isolatioin of **2** and **4** as clusters with V(IV) sites and the $[V_6O_{13}\{(OCH_2)_3CR\}_2]^{2-}$ series as V(V) series.

X-ray Crystal Structures. The structures of the molecular anions of **1–4** possess the gross metal–oxygen framework of the hexametalate core $\{M_6O_{19}\}$, shown in structure I, but perturbed by the influence of the trialkoxy ligands, by protonation of doubly bridging oxo groups, and by reduction of the vanadium centers. The highly symmetrical parent core has been reported for $[Mo_6O_{19}]^{2-}$,[48] $[W_6O_{19}]^{2-}$,[49] and $[Ta_6O_{19}]^{8-}$,[50] and more or less distorted cores have been observed for a variety of derivatized clusters, such as $[V_6O_{13-n}(OH)_n\{(OCH_2)_3CR\}_2]^{n-}$,[37] $[Fe_6O(OR)_{18}]^{2-}$,[51] $[Mo_6O_{18}(NNR_2)]^{3-}$,[52] $[Mo_6O_{18}(NNR)]^{2-}$,[53] $[Mo_6O_{18}(NR)]^{2-}$,[53,54] $[Mo_6O(OR)_{18}]$,[55] and a variety at species containing the $\{M_6(\mu\text{-}O_6)\}$ unit.[56]

As illustrated in Figure 1, the structures of **1–3** and those of the $[V_6O_{13-n}(OH)_n\{(OCH_2)_3CR\}_2]^{2-}$ series[37] are related to the hypothetical $\{V_6O_{19}\}$ parent by replacement of varying numbers of doubly bridging oxo groups by alkoxy oxygen donors of the polyol ligands. The substitution pattern adopted by the ligands reflects the steric requirements of the trialkoxy groups which preferentially bridge three metals in a triangular arrangement. The ligands cap the triangular faces of the tetrahedrral cavities of the hexametalate framework, which are shown schematically in Figure 2. Although there are eight triangular faces associated with the tetrahedral cavities of the $\{V_6O_{19}\}$ core, a maximum of four may be occupied at any one time by the trialkoxy ligands. While an extensive series of clusters symmetrically substituted by two trialkoxide ligands has been described previously,[37] structures **1–4** demonstrate that additional substitution patterns may be achieved by exploiting the potential of hydrothermal synthesis to induce crystal growth of reduced phases.

The structure of **1** revealed the presence of Ba^{2+} cations and discrete molecular anions $[V_6O_7(OH)_3\{(OCH_2)_3CCH_3\}_2]^{2-}$, shown in Figure 3. The structure of **1** is related to that of $\{V_6O_{19}\}$ by substitution of nine doubly-bridging oxo groups by bridging alkoxy oxygen donors of the three ligands associated with the cluster.

(48) Nagano, O.; Sasaki, Y. *Acta Crystallogr.* **1979**, *B35*, 387.
(49) Fuchs, J.; Freiwald, W.; Hartl, H. *Acta Crystallogr.* **1978**, *B34*, 1764.
(50) Aronsson, B. *Ark. Kem* **1954**, *7*, 49.
(51) Hegetschweiler, K.; Schmalle, H. W.; Streit, H. M.; Gramlich, V.; Hund, H. U.; Erni, I. *Inorg. Chem.* **1992**, *31*, 1299; Hegetschweiler, K.; Schmalle, H.; Streit, H. M.; Schneider, W. *Inorg. Chem.* **1990**, *29*, 3625.
(52) Bank, S.; Ku, S.; Shaikh, S. N.; Sun, X.; Zubieta, J. *Inorg. Chem.* **1988**, *27*, 3535 and references therein. Hsieh, T.-C.; Zubieta, J. *Polyhedron* **1985**, *5*, 1655.
(53) Kang, H.; Zubieta, J. *J. Chem. Soc., Chem. Commun.* **1988**, 1192.
(54) Du, Y.; Rheingold, A. L.; Maatta, E. A. *J. Am. Chem. Soc.* **1992**, *114*, 345.
(55) Hollingshead, J. A.; McCarley, R. E. *J. Am. Chem. Soc.* **1990**, *112*, 7402.
(56) Schmid, R.; Mosset, A.; Galy, J. *Inorg. Chim. Acta* **1991**, *179*, 167 and references therein.

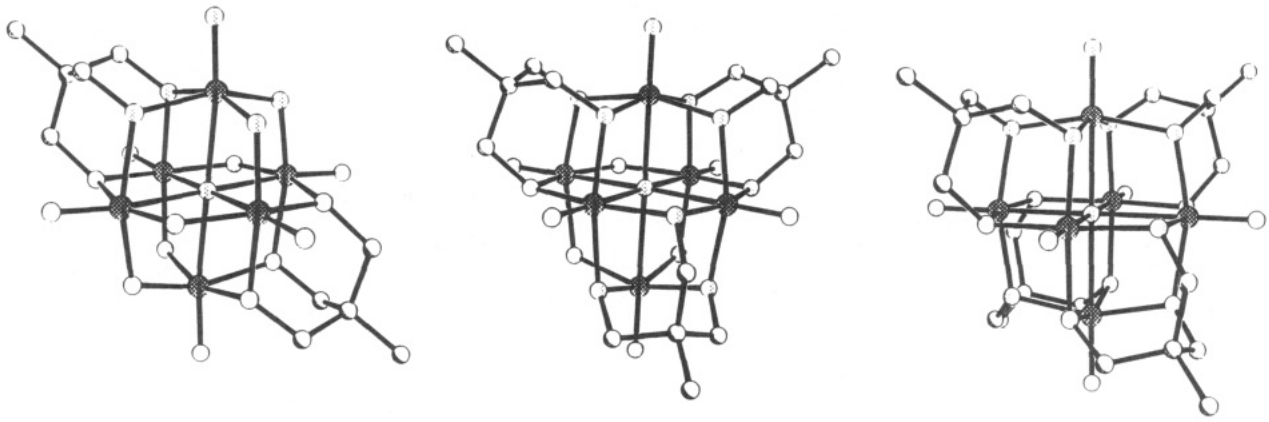

Figure 1. Schematic representations of the structures of (left to right) (a) $[V_6O_{13}\{(OCH_2)_3CCH_3\}_2]^{2-}$, (b) $[V_6O_7(OH)_3\{(OCH_2)_3CCH_3\}_3]^{2-}$, and (c) $[V_6O_7\{(OCH_2)_3CCH_2CH_3\}_4]^{2-}$. The point symmetries are C_{2h}, C_{3v} and T, respectively.

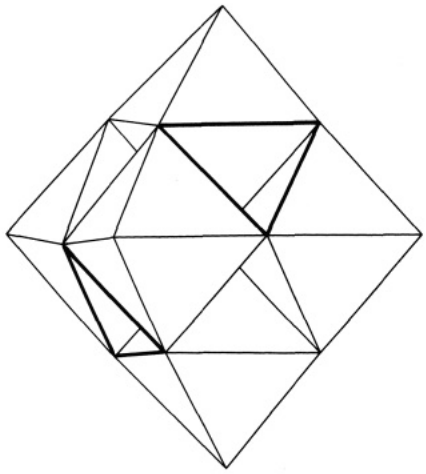

Figure 2. Polyhedral representation of the hexametalate core, highlighting the triangular cavities available for the trialkoxy ligands.

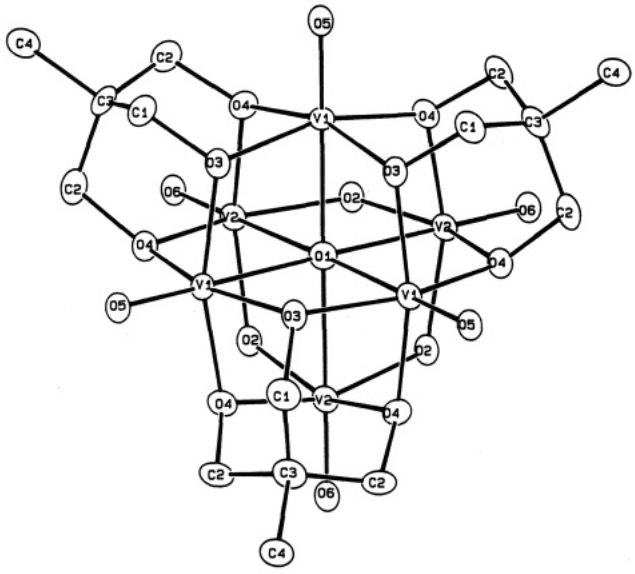

Figure 3. Perspective view of the anion of **1**, showing the atom-labeling scheme.

The oxidation state assignment of cluster **1** is consistent with potentiometric titrations which show six V(IV) sites and with valence sum calculations.[57] This assignment requires that the doubly bridging oxygen atoms be in the protonated hydroxy form. The V(2)–O(4) distances of 2.00(1) Å are consistent with this assignment, since doubly-bridging oxo groups in reduced vanadium clusters exhibit distances of 1.87(1) Å,[37] while doubly-bridging hydroxy groups fall in the range 1.97–2.00 Å, as illustrated in Table VII.

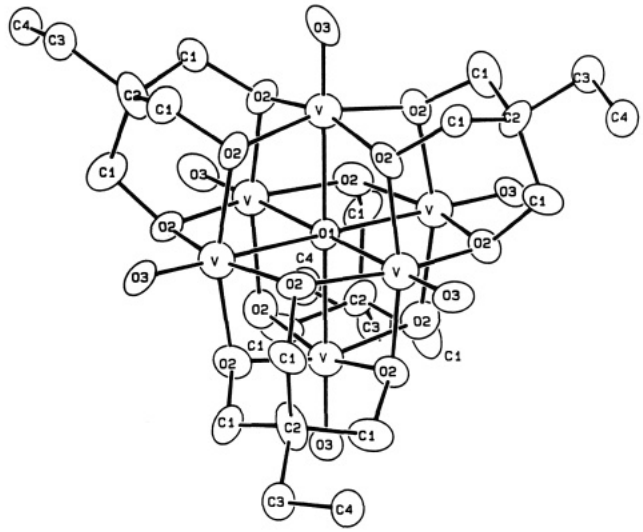

Figure 4. Perspective view of the anion of **2**, showing the atom-labeling scheme.

While the gross structural features of the anion of **3** are similar to those of **1**, the structures differ in the overall cluster oxidation states. Potentiometric titrations and valence sum calculations on **3** reveal that the species is a mixed valence cluster with five V(IV) sites and one V(V) site. The valence sum calculations provide a valence of 3.9 valence units (vu) for V(1) and 4.3 vu for V(2), suggesting that the V(V) site is averaged about the $\{V(2)\}_3$ face of the cluster.

The structure of the molecular anion of **2**, shown in Figure 4, exhibits the $\{V_6O_{19}\}$ core, with substitution of all twelve doubly-bridging oxo-groups by doubly bridging alkoxy donors. The structural parameters associated with the anions of **1–3** are compared to those of the $[V_6O_{13-n}(OH)_n\{(OCH_2)_3CR\}_2]^{2-}$ series in Table XI. The most obvious geometric consequences of substitution of alkoxy groups for oxo-groups and of reduction of the vanadium sites are manifested in core expansion. Figure 5 provides a schematic representation of the $\{V_6O_{19}\}$ core viewed as planar layers of negatively charged close-packed oxygen atoms separated by layers of vanadium atoms, while Table XII tabulates the interplanar separations for the series of $\{V_6O_{19}\}$ structural types studied to date.

An unusual property of reduced vanadium oxide clusters is their tendency to form cages encapsulating either negative ions[58,59]

(57) Brown, I. D.; Wu, K. K. *Acta Crystallogr.* **1976**, *B32*, 1957.

(58) Müller, A.; Penk, M.; Rohlfing, R.; Krickemeyer, E.; Döring, J. *Angew. Chem., Int. Ed. Engl.* **1990**, *29*, 926.

Table XI. Comparison of Structural Parameters for Clusters with the $\{V_6O_{19}\}$ and $\{V_6FO_{18}\}$ Cores

	V–O				
	bridging oxo	bridging hydroxy	bridging alkoxy	central oxo (fluoro)	ref
$[V_6O_{13}\{(OCH_2)_3CCH_3\}_2]^{2-}$	1.823		2.022	2.242	37
$[V_6O_{11}(OH)_2\{(OCH_2)_3CCH_3\}_2]$	1.823	1.879	1.994, 2.019	2.219, 2.253	37
$[V_6O_{10}(OH)_3\{(OCH_2)_3CNO_2\}_2]^{2-}$	1.86	1.94	2.017	2.28	
$[V_6O_9(OH)_4\{(OCH_2)_3CCH_3\}_2]^{2-}$	1.869	1.946	2.004, 2.038	2.287	37
$[V_6O_7(OH)_6\{(OCH_2)_3CCH_3\}_2]^{2-}$		1.994	2.004	2.038	37
$[V_6O_7(OH)_3\{(OCH_2)_3CCH_3\}_3]^{2-}$ (**1**)		1.999	1.973, 2.074	2.272, 2.328	this work
$[V_6O_7\{(OCH_2)_3CCH_2CH_3\}_4]^{2-}$ (**2**)			2.007	2.315	this work
$[V_6O_7(OH)_3\{(OCH_2)_3CCH_3\}_3]^{1-}$ (**3**)		1.974	1.976, 2.006	2.236, 2.382	this work
$[V_6O_6F(OH)_3\{(OCH_2)_3CCH_3\}_3]^{1-}$ (**4**)		2.037	1.955, 2.045	2.245, 2.522 (F)	this work

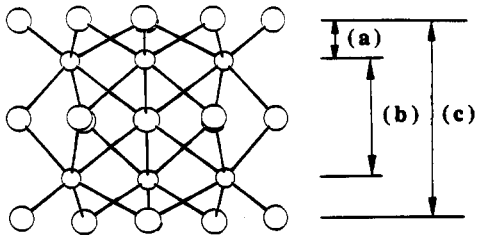

Figure 5. Schematic representation of the $\{V_6O_{19}\}$ core viewed as planar layers of negatively charged close-packed oxygen atoms separated by planes of vanadium cations.

Table XII. Distances between Planes Defined in Figure 5 for Structures with the $\{V_6O_{19}\}$ and $\{V_6FO_{18}\}$ Cores

	a	b	c
$[V_6O_{19}\{Rh(C_5Me_5)\}_4]$	0.89	2.59	4.40
$[V_6O_{13}\{(OCH_2)_3CCH_3\}_2]^{2-}$	1.01	2.36	4.36
$[V_6O_{11}(OH)_2\{(OCH_2)_3CCH_3\}_2]$	1.00	2.40	4.39
$[V_6O_{10}(OH)_3\{(OCH_2)_3CNO_2\}_2]^{2-}$	0.98	2.54	4.49
$[V_6O_9(OH)_4\{(OCH_2)_3CCH_3\}_2]^{2-}$	0.97	2.56	4.50
$[V_6O_7(OH)_6\{(OCH_2)_3CCH_3\}_2]^{2-}$	0.95	2.68	4.59
$[V_6O_7(OH)_3\{(OCH_2)_3CCH_3\}_3]^{2-}$ (**1**)	0.94	2.68	4.59
$[V_6O_7\{(OCH_2)_3CCH_2CH_3\}_4]^{2-}$ (**2**)	0.94	2.67	4.54
$[V_6O_7(OH)_3\{(OCH_2)_3CCH_3\}_3]^{1-}$ (**3**)	0.93	2.69	4.54
$[V_6O_6F(OH)_3\{(OCH_2)_3CCH_3\}_3]^{1-}$ (**4**)	0.94	2.67	4.54

or cations.[42,46] As shown in Figure 6, compound **4** represents a most unusual member of this class of clusters, and the first example to our knowledge of a hexametalate core possessing a central anion other than oxide. The structure of the anion of **4** is grossly similar to those of **1** and **3**. However, the results of the elemental analyses on **4**, the thermal displacements associated with the central atom of the core, and the relevant bond distances identify the central site as fluoride, F^-. The most significant structural distortion consequent to the replacement of the central oxide by fluoride is the displacement of the fluoride toward the triangular face defined by the three V(1) centers. Thus, the V(1)–F distances are 2.245(6) Å, while the V(2)–F distances have lengthened to 2.522(6) Å. The valence sum calculations on **4** are consistent with six V(IV) centers, also confirming the presence of a monoanionic group in place of one oxo ligand. The terminal oxo groups and the bridging hydroxy oxygens exhibit normal structural parameters and temperature factors, again an observation consistent with the identity of the central atom as F^-. The core of **4** may thus be defined as $\{V_6(\mu_3\text{-}F)O_{18}\}$ rather than the common hexametalate core $\{M_6(\mu_6\text{-}O)O_{18}\}$.

While the structures of **1**, **3**, and **4** are isomorphous, the differences in the cell parameters reflect the steric requirements of the various cations. As shown in Figure 7, the cations in all three structures are wedged between pairs of anion clusters. The large Ba^{2+} cation of **1** is effectively nine coordinate, making close contacts with the three –OH oxygens of one cluster, three alkoxy oxygens of a neighboring cluster, and three aquo ligands. The

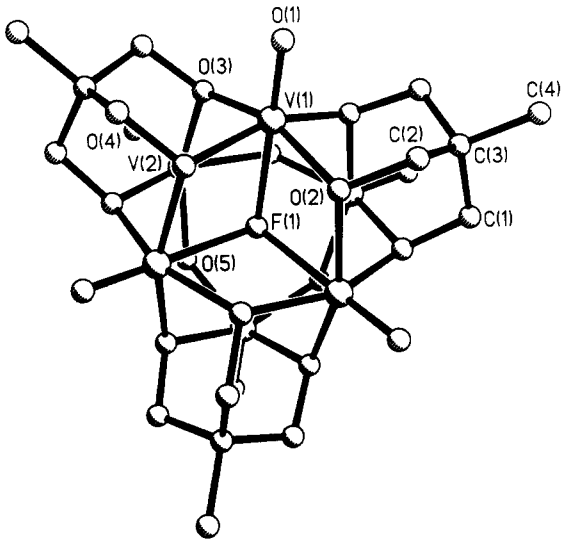

Figure 6. Perspective view of the structure of **4**, showing the atom-labeling scheme.

coordination geometry about the Ba^{2+} is distorted tricapped octahedral.

The Me_3NH^+ cation of **3** occupies the identical lattice site to that of the Ba^{2+} in **1** with the hydrogen directed toward the three –OH groups of one cluster and the methyl groups toward the more hydrophobic pocket provided by the alkoxy-ringed face of the neighboring cluster.

The different coordination requirements of the Na^+ cation compared to Ba^{2+} and $(Me_3NH)^+$ are illustrated in the contrasting details of the extended structures of **1**, **3**, and **4**. The octahedral Na^+ is bonded to three alkoxy oxygens of one cluster and three aquo ligands, which in turn hydrogen bond to the three –OH groups of a neighboring cluster. It should be noted that, in contrast to the coordination mode adopted in **4**, the Na^+ cation of **2** is octahedrrally coordinated to three alkoxy oxygens from each of two neighboring anion clusters.

Magnetism. The high-temperature magnetic susceptibility data ($T > 100$ K) of **1a** exhibits Curie–Weiss paramagnetism

$$\chi = \frac{C}{T-\theta} = \frac{Ng^2\mu_B{}^2S(S+1)}{3k(T-\theta)} \qquad (1)$$

with $C = 1.66$ (emu-K)/mol, $\theta = -69.8$ K, and TIP = 0.00386 emu/mol. The electron structure of $Rb_2[V_6O_7(OH)_3\{(OCH_2)_3CCH_3\}_3]$ (**1a**) corresponds to one unpaired electron per vanadium. This results in an average Curie–Weiss g value of $g = 1.72$ for each of the six V(IV) ions in the cluster.

At lower temperatures an anomaly is observed in the temperature dependence of the magnetic susceptibility data. As the temperature is lowered to around 40 K, the magnetic susceptibility of the sample passes through a broad maximum and begins to decrease at lower temperatures. This behavior is expected for short-range antiferromagnetic exchange and is consistent with magnetic exchange within the vanadium hexamer with the six vanadium(IV) ions occupying the corners of an octahedron.

(59) Müller, A.; Doring, J. *Z. Anorg. Allg. Chem.* **1991**, *595*, 251.
(60) O'Connor, C. J. *Prog. Inorg. Chem.* **1982**, *29*, 203.

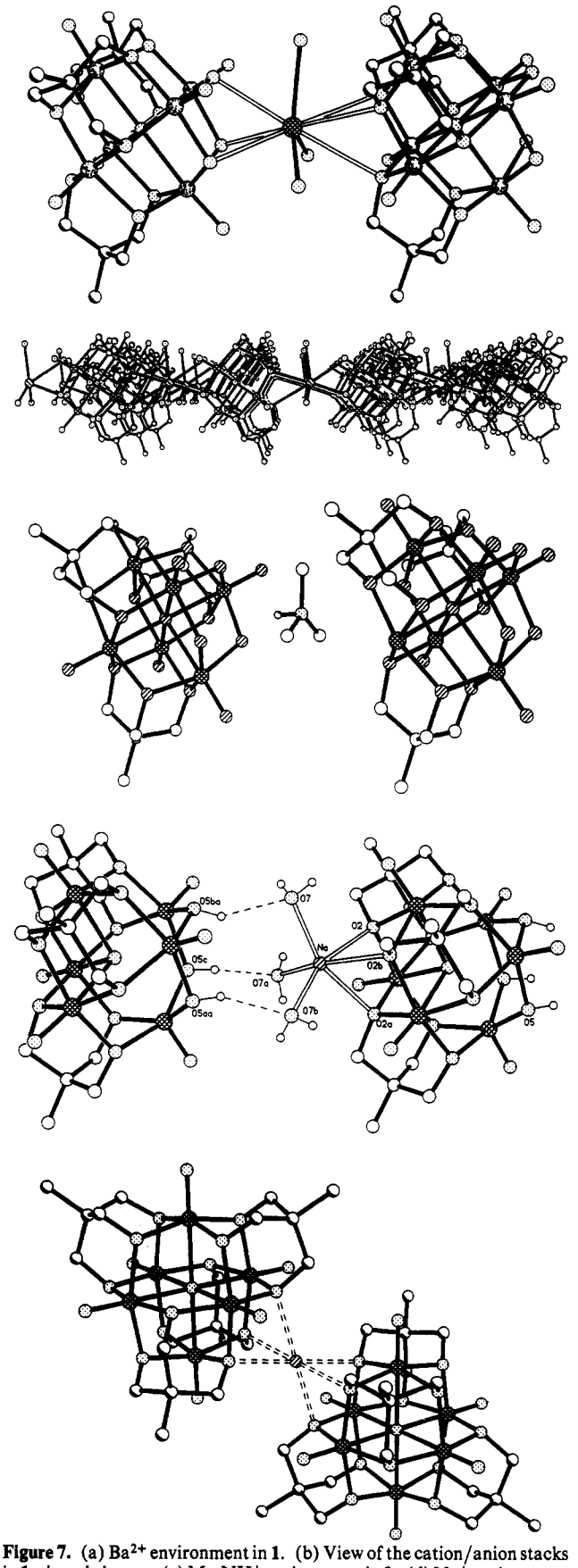

Figure 7. (a) Ba^{2+} environment in **1**. (b) View of the cation/anion stacks in **1**, viewed along a. (c) Me_3NH^+ environment in **3**. (d) Na^+ environment in **4**. (e) Na^+ environment in **2**. The structures are depicted top to bottom.

The magnetic exchange that is expected in vanadium(IV) with a ^2D free ion ground term, d^1 electron structure, and spin S = $^1/_2$ is the isotropic Heisenberg spin Hamiltonian.

$$H = -2JS_iS_j \qquad (2)$$

Within the context of the crystal structure of this material, the exchange from this spin Hamiltonian may be propagated via an isotropic octahedral six atom cluster magnetic exchange interaction. Since the hexamer may be approximated as an octahedron,

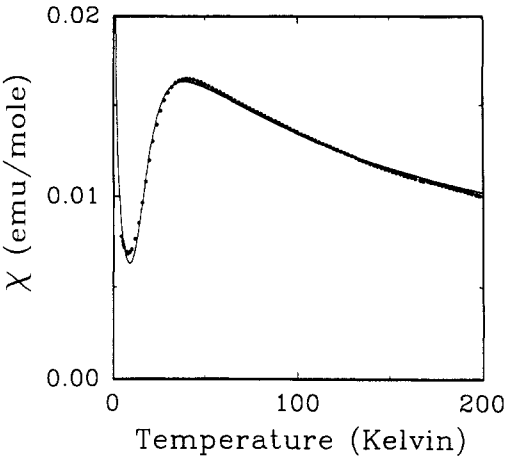

Figure 8. Magnetic susceptibility of $Rb_2[V_6O_7(OH)_3\{(OCH_2)_3CCH_3\}_3]$ (**1a**) plotted as a function of temperature over the 6–200 K temperature region. The curve drawn through the data is the fit to the isotropic, symmetric hexamer magnetic exchange model as described in the text.

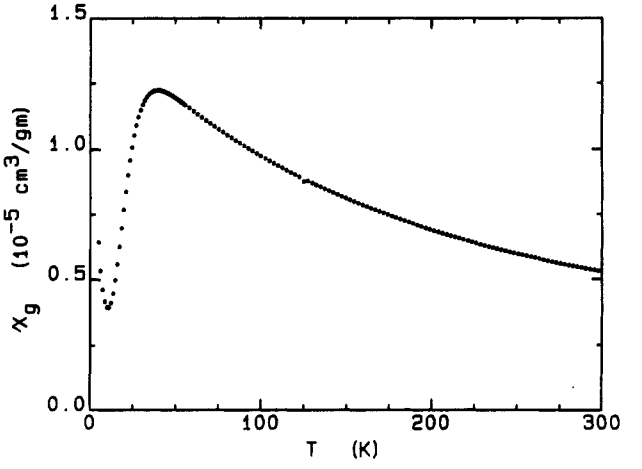

Figure 9. Magnetic susceptibility of $Na_2[V_6O_7\{(OCH_2)_3CCH_2CH_3\}_4]$ (**2**) plotted as a function of temperature over the 6–300 K temperature range.

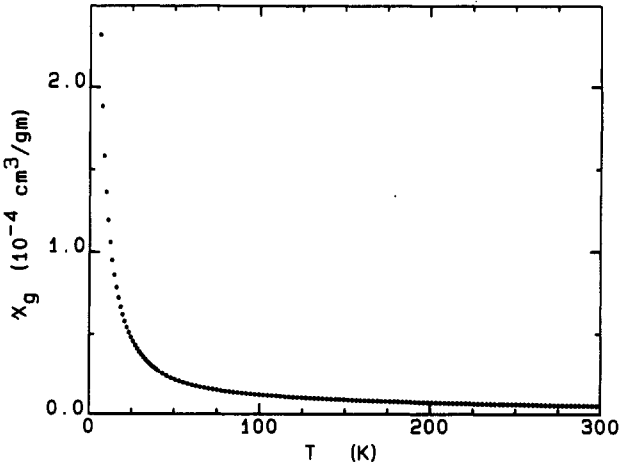

Figure 10. Magnetic susceptibility of $(Me_3NH)[V_6O_7(OH)_3\{(OCH_2)_3CCH_3\}_3]$ (**3**) plotted as a function of temperature over the 6–300 K temperature range.

a summation may be taken over all possible V(IV)–V(IV) interactions within the cluster and all J values are restrained to be the same.

The behavior of the totally isotropic and symmetric six atom spin $S = {}^1/_2$ magnetic exchange may be described by the following magnetic susceptibility equation

$$\chi = \frac{Ng^2\mu_B{}^2}{kT}\left(\frac{56e^{2x} + 200e^{6x} + 196e^{12x} + 60e^{20x}}{14 + 84e^{2x} + 100e^{6x} + 49e^{12x} + 9e^{20x}}\right) \quad (3)$$

where the magnetic susceptibility is calculated per hexamer unit, $x = J/kT$, and all of the other parameters have their usual meaning.

The magnetic susceptibility data recorded at the lowest temperatures indicated the presence of a paramagnetic impurity. The magnetic susceptibility data were fit over the entire temperature region to the isotropic, symmetric hexamer magnetic exchange model (eq 3) corrected for the presence of the paramagnetic impurity. The fitted parameters are $g = 1.88$, $J/k = -32.1$ K, and TIP = 0.00329 emu/mol, with a 1.2% paramagnetic impurity. The smooth line drawn through the data points in Figure 8 is the theoretical curve calculated from eq 3 with the parameters indicated. The magnetic properties of **1** are similar to those of **1a**, with a room temperature moment consistent with six unpaired spins and an antiferromagnetic transition at 38K.

The magnetic properties of **2** are similar to those of **1a** as shown in Figure 9. Compound **2** exhibits an average Curie–Weiss g value of 1.74 for each of six V(IV) sites in the cluster. As the temperature is lowered to 38 K, the magnetic susceptibility passes through a broad maximum and begins to decrease at lower temperatures. Again, this behavior is characteristic for short range antiferromagnetic exchange.

The magnetic properties of **3** are quite distinct from those of **1a** and **2** as shown in Figure 10. Compound **3** exhibits an average Curie–Weiss g-value of 1.67 for each of five V(IV) sites in the cluster. The magnetic moment decreases from this value to 1.27 μ_B at 40 K, indicating net antiferromagnetic coupling. No maximum in the magnetic behavior of **3** is observed in the range 5–300 K.

Acknowledgment. This work was supported by NSF Grant No. CHE9119910.

Supplementary Material Available: Tables of experimental details and crystal parameters, bond lengths and angles, anisotropic temperature factors, and calculated hydrogen atom positions for structures **1–4** (27 pages). Ordering information is given on any current masthead page.